

3-D resistivity inversion with electrodes displacements

M.H.Loke*

Geotomosoft Solutions
Penang, Malaysia
drmhloke@yahoo.com

P.B.Wilkinson

British Geological Survey
Nottingham, U.K.
pbw@bgs.ac.uk

J.E.Chambers

British Geological Survey
Nottingham, U.K.
jecha@bgs.ac.uk

SUMMARY

3-D resistivity monitoring surveys are used to detect temporal changes in the subsurface using the measurements repeated over the same site. The positions of the electrodes are measured at the start of the survey program and perhaps at occasional intervals. In areas with unstable ground, the positions of the electrodes can be displaced by ground movements. If this occurs at times when the positions of the electrodes are not measured, they have to be estimated from the resistivity data. The smoothness-constrained least-squares optimisation method can be modified to include the electrodes positions as additional unknown parameters. 3-D resistivity surveys present a special challenge due to the greater computational requirements for the forward modelling routine and the possible movements of the electrodes in three directions. To reduce the calculation time, a fast adjoint-equation method is used to calculate the Jacobian matrices required by the least-squares method. It is several orders of magnitude faster than the simpler perturbation method previously used for 2-D problems. In areas with large near-surface resistivity contrasts, the inversion routine sometimes cannot accurately distinguish between electrodes displacements and subsurface resistivity variations. To overcome this problem, the model for the initial time-lapse data set (with accurately known electrodes positions) is used as the starting model for the inversion of the later-time data set. This greatly improves the accuracy of the estimated electrode positions compared to the use of a homogeneous half-space starting model.

Key words: 3-D, resistivity, inversion, electrode, displacements.

INTRODUCTION

Geoelectrical monitoring surveys are frequently used to detect temporal changes in the subsurface resistivity (Loke *et al.*, 2014). The measurements are repeated a number of times using the same electrodes layout. The electrode positions are usually accurately measured at the start, and thereafter possibly at intervals. Ground movements sometimes occur between the times of electrode positions measurements and thus are not accurately known for some data sets. It is necessary to determine the changes in the electrodes positions from the resistivity data itself (Wilkinson *et al.*, 2015; 2016). A method was presented by Kim (2014) where both the subsurface resistivity and electrodes positions are unknown variables to be determined by the least-squares optimisation method for 2-D surveys. However a relatively slow method was used to calculate the Jacobian matrix of partial derivatives that is impractical for 3-D surveys. A second problem faced was that a relatively large damping factor for the electrodes positions vector was required to reduce distortions in the calculated surface profile due to near-surface resistivity variations. In this paper, we describe a fast method to calculate the Jacobian matrix and a modified inversion algorithm to reduce the distortions.

METHOD AND RESULTS

Nonlinear least-squares optimisation method

The smoothness-constrained least-squares optimisation method is frequently used for 2-D and 3-D inversion of resistivity data. The modified least-squares equation (Kim, 2014) where the electrodes positions are included as model parameters can be written as

$$[G_i^T R_d G_i + \lambda_i^2 V^T R_m V] \Delta q_i = G_i^T R_d g_i - \lambda_i V^T R_m V q_{i-1} \quad (1)$$

where

$$q = \begin{pmatrix} r \\ x \\ y \\ z \end{pmatrix}, G = \begin{pmatrix} J \\ X \\ Y \\ Z \end{pmatrix}, V = \begin{pmatrix} W \\ \alpha W_x \\ \beta W_y \\ \gamma W_z \end{pmatrix}.$$

The Jacobian matrix G consists of J (the model resistivity sensitivity values) together with the X , Y and Z (sensitivity values for the changes in the x , y and z electrodes positions) matrices. λ is a damping factor vector and g is the data misfit vector. q is the model parameters vector consisting of r (logarithm of model resistivity) and x , y and z (electrodes positions) vectors. Δq_i is the change in the model parameters. W is the resistivity spatial roughness filter term. W_x , W_y and W_z are the roughness filters for the electrodes positions vectors. R_d and R_m are weighting matrices used by the L1-norm inversion method (Loke *et al.*, 2003). α , β and γ are the relative damping factors for the electrodes positions vectors. A homogeneous half-space is commonly used as the starting model for the optimisation algorithm. In a time-lapse survey the initial positions of the electrodes are usually accurately measured and can be treated as fixed parameters in the inversion of the initial data set. The temporal changes in the subsurface resistivity are usually much less than the spatial variations (Loke *et al.*, 2014). Thus the inversion model of the initial data set provides a good starting model for the later time data sets. We modify the inversion algorithm to use the model from a previous survey as the starting model.

Calculation of the Jacobian matrix using the adjoint-equation method

The potentials are calculated by solving the following finite-element capacitance matrix equation (Silvester and Ferrari, 1990).

$$\mathbf{C}\Phi = \mathbf{s} \quad (2)$$

Φ is a vector with the potentials at the nodes of the mesh while \mathbf{s} is the current source vector. \mathbf{C} is the capacitance matrix that contains the positions of the nodes and model conductivity values. The \mathbf{C} matrix is a symmetric sparse matrix with 28 non-zero sub-diagonals for 3-D linear hexahedral elements (Figure 1a). Kim (2014) used the perturbation method to calculate the necessary partial derivatives for changes in the electrodes positions. For example, a change in the x -position of electrode number 5 is approximated by

$$\frac{\partial \phi_i}{\partial x_5} \approx \frac{\phi_i(x_5 + \Delta x_5) - \phi_i(x_5)}{\Delta x_5} \quad (3)$$

For a survey grid with e electrodes it will be necessary to calculate the potentials by resolving equation (2) $3e$ times. While using the perturbation method is possible for 2-D problems, it becomes impractical for 3-D problems where the forward modeling routine is about two to three orders of magnitude slower. We use a modification of the adjoint-equation approach (McGillivray and Oldenburg, 1990) to calculate the \mathbf{X} , \mathbf{Y} and \mathbf{Z} Jacobian matrices. For example, by differentiating equation (2) with respect to z_k , the derivative of the potential values ($\partial \Phi / \partial z_k$) due to a shift in the z direction for the electrode number k is as follows.

$$\mathbf{C} \frac{\partial \Phi}{\partial z_k} = - \frac{\partial \mathbf{C}}{\partial z_k} \Phi \quad (5)$$

It is only necessary to calculate the non-zero terms in the $\partial \mathbf{C} / \partial z_k$ matrix as this equation has the same form as (2). Figure 1b shows an overhead view of part of the 3-D finite-element mesh. A shift in the position of one electrode (5) will only affect the nodes that lie between the adjacent electrodes (1 to 9). If the finite-element mesh has n_z nodes in the z direction, the number of nodes affected will be $81n_z$. This is much smaller the full finite-element mesh that can have tens of thousands to millions of nodes. The elements of the \mathbf{C} matrix have the following form (Silvester and Ferrari, 1990).

$$c_{pqr} = k_{pqr}(x, y, z) \sigma_j \quad (6)$$

where σ_j is the model cell conductivity. The function $k_{pqr}(x, y, z)$ depends only on the coordinates of the nodes at the corners of the hexahedral element. The change in the coupling coefficients are calculated numerically using a two-sided finite-difference formula as follows.

$$\frac{\partial c_{pqr}}{\partial z_k} \approx \frac{k_{pqr}(x, y, z_k + \Delta z_k) - k_{pqr}(x, y, z_k - \Delta z_k)}{2\Delta z_k} \sigma_j \quad (7)$$

The two-sided formula avoids the directional bias in a one-sided formula such as (3). The time required to calculate the $k_{pqr}(x, y, z)$ terms is negligible compared to resolving equation (2) as required by the perturbation method. The partial derivative vector $\partial \Phi / \partial z_k$ values are calculated by multiplying the non-zero elements in the $\partial \mathbf{C} / \partial z_k$ matrix with the net potentials at the nodes due to current sources at the positions of the current electrodes used in the measurement. The resulting vector is then multiplied by the net potentials at the nodes due to current sources at the positions of the potential electrodes. The required potentials are already available in the process of solving (2) to calculate the apparent resistivity values.

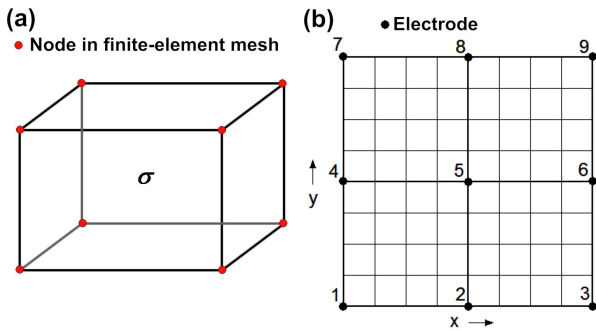


Figure 1: (a) Hexahedral element with 8 nodes. (b) Overhead view of the top section of the mesh around electrode 5.

Synthetic model example

We show the results for a synthetic model that provides an objective test of the inversion method as the true positions of the electrodes and resistivity values are known. Figure 2a shows the 3-D test model. The initial model has the electrodes arranged in a 29 by 13 rectangular grid with the electrodes 1 metre apart on a flat surface. The background medium has a resistivity of 100 ohm.m. There are two bands of low (30 ohm.m) and high (300 ohm.m) resistivity to demonstrate the effect of large near surface anomalies on the inversion. There is a small near surface high resistivity rectangular prism (400 ohm.m) and a deeper low resistivity prism (20 ohm.m). In the perturbed model, 3 of the electrodes are shifted horizontally and 1 electrode vertically (Figure 2b). The resistivities of the small rectangular prisms are also changed to 25 and 350 ohm.m to simulate changes in the subsurface resistivity. The test data set consists of all the possible inline dipole-dipole measurements along the x and y directions with a maximum geometric factor of 1056 m (corresponding to a dipole-dipole array with $a=1$ m and $n=6$). This gives a total of 6573 data points. Voltage dependent Gaussian random noise (Zhou and Dahlin, 2003) with a mean amplitude of 4 milliohm was added to the data before they were converted to apparent resistivity values. The average noise level for the resulting apparent resistivity data set is 1.1%. Figure 3 shows the inversion models for the initial and perturbed data sets with fixed electrodes in a rectangular grid. The inversion model has 8 layers but only the first 5 layers are shown as there are no significant resistivity variations in the deeper layers. The L1-norm method was used for both

the data misfit and model roughness (Loke *et al.*, 2003). The model for the initial data set closely matches the true structure (Figure 3a) with a data misfit of 1.2% which is slightly above the noise level added. The model for the perturbed data set show significant distortions at the positions of the 4 shifted electrodes (Figure 3b) and a higher data misfit of 1.8%. Figure 4 shows the inversion models obtained when the electrodes positions are allowed to change during the inversion using different values for electrodes relative damping factors (α, β, γ). The data misfit is similar to the added noise level with damping factors of 1 and 5. Using a high damping factor of 50 essentially fixes the electrodes positions (Figure 4c) giving a model similar to that in Figure 3b with fixed electrodes. The recovered electrodes grid shows significant distortions with a damping factor of 1. It is expanded outwards along the y -direction over the low resistivity band and compressed inwards over the high resistivity band. This is probably because an increase in the spacing between the electrodes reduces the measured resistance value in a similar way as a decrease in the resistivity. The distortions are greatly reduced with a damping factor of 5. Figure 5a shows the x - z surface profile along the $y=10$ m line that crosses electrode 4 (Figure 2b) that was shifted upwards. The profile with a damping factor of 1.0 shows significant distortions that is greatly reduced when it is increased to 2.5, and almost completely eliminated with a value of 5.0. Figure 6 shows the results obtained when the model for the initial data set (Figure 3a) is used as the starting model for the inversion of the perturbed data set. The distortions with the lowest damping factor of 1.0 is greatly reduced (Figures 5b and 6a) and almost completely eliminated with a damping value of 2.5 (Figure 5b). Using the model for the initial data set essentially carries out the inversion using the change in the apparent resistivity values which removes the effect of the common background resistivity structures.

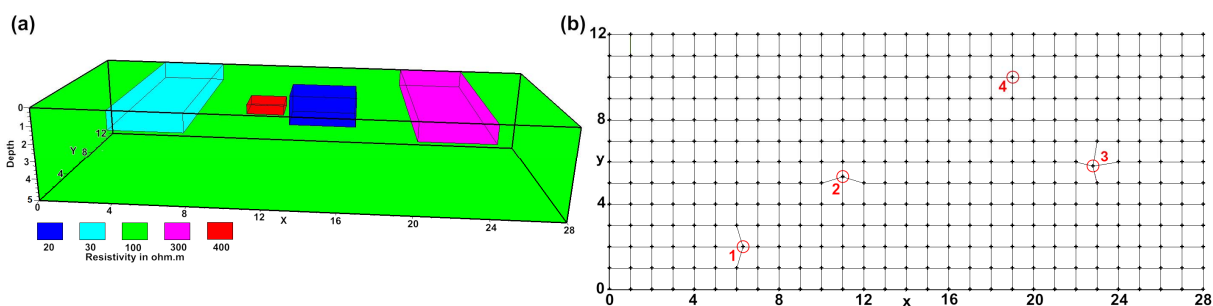


Figure 2: (a) 3-D synthetic test model with a rectangular survey grid. In the perturbed model, the resistivities of the smaller blocks were changed from 400 and 20 ohm.m to 350 and 25 ohm.m. (b) The survey grid for the perturbed model. The four electrodes shifted are marked by red circles. Electrode 1 was shifted 0.3 m in the x -direction, electrode 2 moved 0.3 m in the y -direction, electrode 3 moved -0.2 m in both x and y -directions while electrode 4 was shifted vertically upwards by 0.4 m.

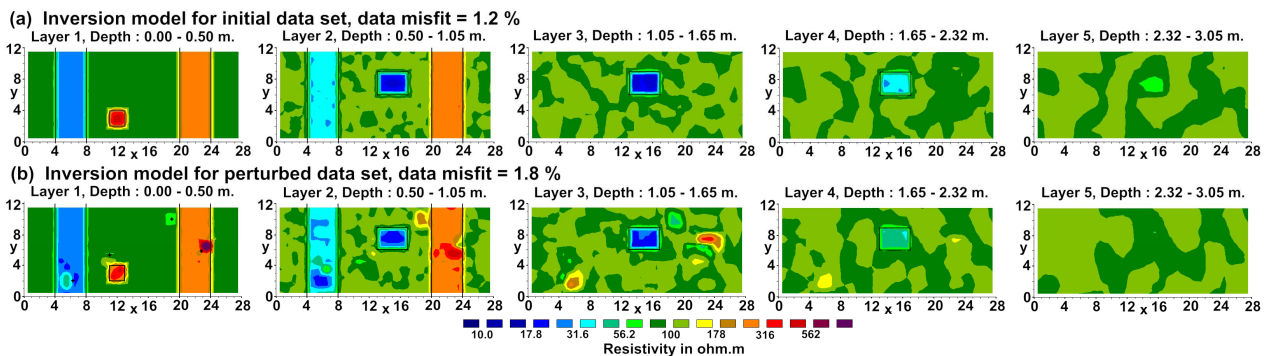


Figure 3: Inversion models for the (a) initial and (b) perturbed data sets with fixed electrodes in a rectangular grid. The true positions of the bands and prisms are marked by black lines. The positions of the shifted electrodes are marked by small crosses in the top layer in (b).

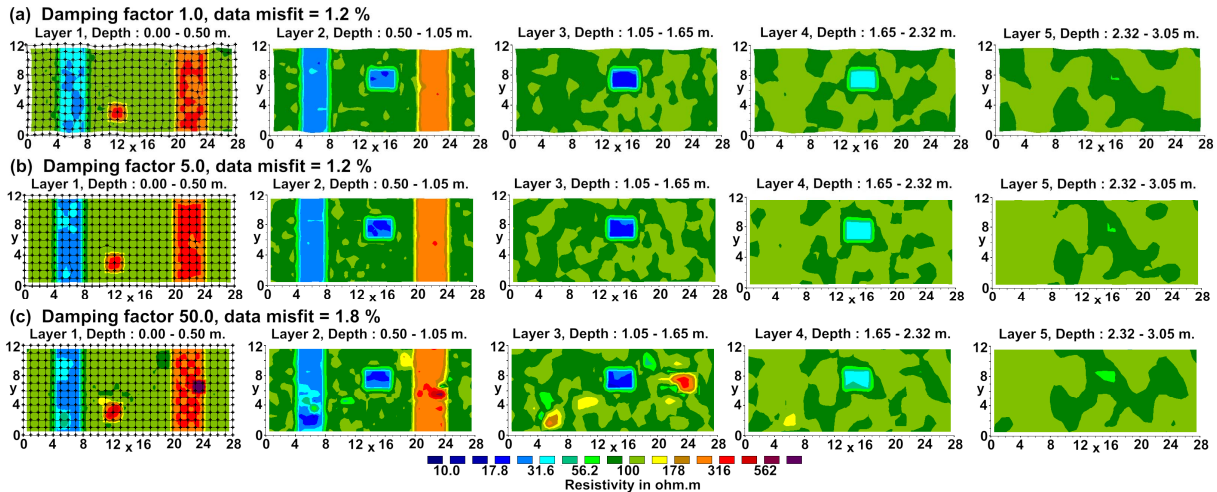


Figure 4: Inversion models for the perturbed data set using different relative damping factors for the electrodes positions vector with a homogenous half-space starting model.

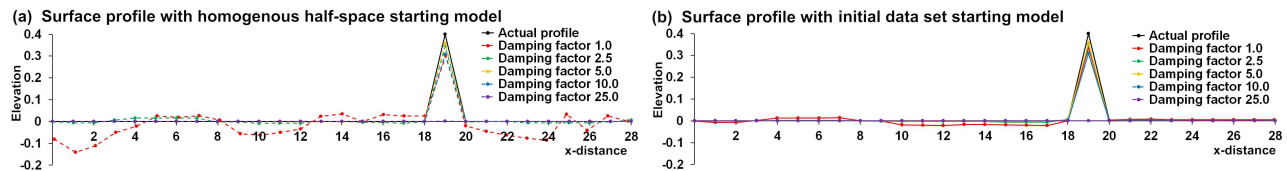


Figure 5: Surface x - z profiles along the line $y=10$ m for inversions using a (a) homogenous half-space and (b) initial data set starting models.

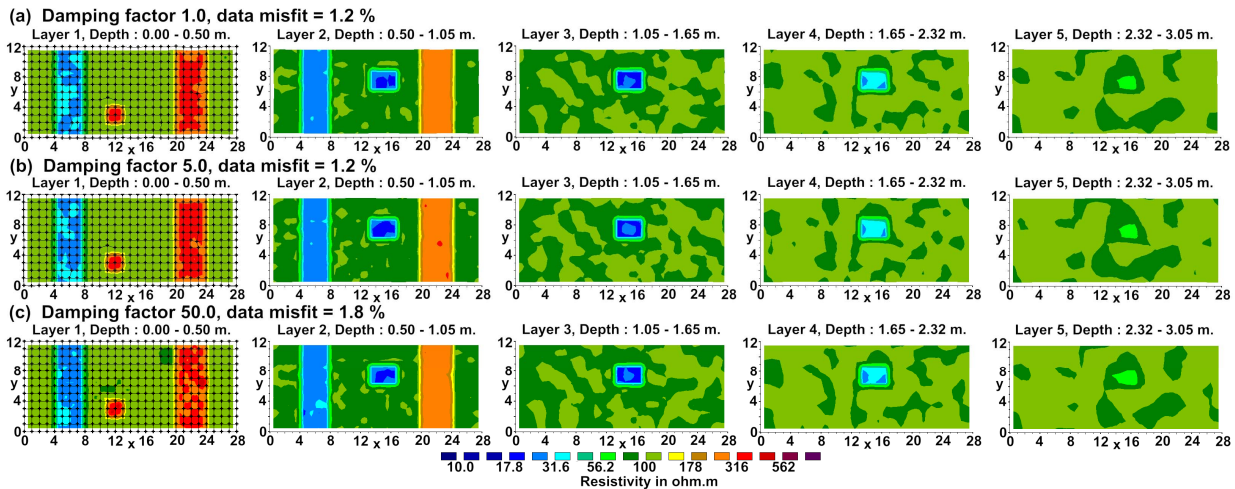


Figure 6: Inversion models for the perturbed data set using different relative damping factors for the electrodes positions vector with the inversion model from the initial data set as the starting model.

CONCLUSIONS

We present a fast technique to calculate the Jacobian matrix for shifts in the electrodes positions using the adjoint-equation method. Using the inversion model for the initial data set with known electrode positions as the starting model for a later data set greatly reduces distortions in the profile caused by subsurface resistivity variations giving more accurate calculated electrodes positions.

REFERENCES

Kim, J.H., 2014. Simultaneous Inversion of Resistivity Structure and Electrode Locations in ERT: 20th European Meeting of Environmental and Engineering Geophysics, Athens, Greece, 14-18 September 2014, We Olym 10.

- Loke M.H., Acworth, I. and Dahlin, T., 2003. A comparison of smooth and blocky inversion methods in 2D electrical imaging surveys: *Exploration Geophysics*, 34, 182-187.
- Loke, M.H., Dahlin, T., Rucker, D.F., 2014. Smoothness-constrained time-lapse inversion of data from 3-D resistivity surveys: *Near Surface Geophysics*, 12, 5-24.
- McGillivray, P. R. and Oldenburg, D. W., 1990. Methods for calculating fr chet derivatives and sensitivities for the non-linear inverse problem : a comparative study: *Geophysical Prospecting*, 38, 499-524.
- Silvester, P.P. and Ferrari, R.L., 1990. *Finite elements for electrical engineers* (2nd. ed.): Cambridge University Press.
- Wilkinson, P.B., Uhlemann, S., Chambers, J.E., Meldrum, P. I. and Loke, M.H., 2015. Development and testing of displacement inversion to track electrode movements on 3D Electrical Resistivity Tomography monitoring grids: *Geophysical Journal International*, 200, 1566-1581.
- Wilkinson, P.B., Chambers, J.E., Uhlemann, S., Meldrum, P.I., Smith, A., Dixon, N. and Loke, M.H., 2016. Reconstruction of landslide movements by inversion of 4-D electrical resistivity tomography monitoring data: *Geophysical Research Letters*, 43, doi:10.1002/2015GL067494
- Zhou, B. and Dahlin, T., 2003. Properties and effects of measurement errors on 2D resistivity imaging surveying: *Near Surface Geophysics*, 1, 105-117.